DIGITAL TOMOGRAPHY INCORPORATING A PRIORI INFORMATION

K. C. Tam and L. J. Thomas III

GE Corporate Research and Development
P.O. Box 8
Schenectady, NY 12301

INTRODUCTION

The technique of tomography has long been used in radiography and in nuclear medicine to sharpen images of objects on the tomographic plane and to blur images of objects on the off-planes. The method is illustrated in Figure 1. Suppose one is interested in examining the plane *T* in the object. The x-ray source and the film are moved parallel to each other in the opposite directions with the plane of interest as the fulcrum. This is achieved by choosing the velocity v_1 of the x-ray source and the velocity v_2 of the film such that the ratio v_1/v_2 is equal to d_1/d_2, where d_1 is the source-to-plane distance, and d_2 is the plane-to-film distance. The objects on the plane of interest are in focus, whereas the objects on the other planes are out of focus and blurred. However, the blurrings could become quite serious in some cases and interfere with the objects of interest.

The method of tomography was modified and applied to the x-ray imaging of multilayered structures under the name of digital tomography (DT) or laminography [1,2,3]. In this paper it is shown that digital tomography is basically a limited-angle imaging problem. Therefore the techniques of limited-angle image reconstructions can be applied to remove the blurrings on the tomographic planes caused by the densities on the adjacent planes. This method significantly improves image quality for the inspection of closely spaced layers like those found in multilayer printed circuit boards. Compared to the conventional DT reconstruction method, the new approach:

1. Reduces the blurrings caused by the objects on the off-focus planes

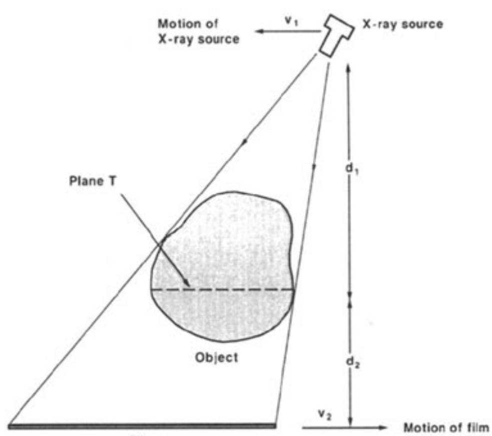

Figure 1. Tomography.

2. Eliminates the edge fall-off effect present with the conventional reconstructions
3. Tolerates close spacing of overlaying planes and reduces the artifacts of strongly attenuating overlaying structures

In the sections that follow, the theory of the conventional DT reconstruction as applied to x-ray scanning is reviewed, and the approach incorporating limited-angle image reconstructions is described in detail. Image reconstructions by the two methods using simulated data are also presented and compared.

CONVENTIONAL DIGITAL TOMOGRAPHY

In digital tomography the radiographs of an object are taken at a number of angles. The DT image of any point P in the object is obtained by

1. Determining for each radiograph, the location of the end-point of the ray from the x-ray source that passes through the point P
2. Summing together the radiograph intensity at these locations

The procedure is illustrated in Figure 2. The resulting images are called tomograms. DT scanning can be carried out using either a linear detector array or a 2-dimensional detector array. In the following discussion, a linear detector array is assumed. The scanning is done in the $x-z$ plane, as shown in Figure 2, with the linear detector array lying parallel to the x dimension. Each $x-z$ plane of the object is scanned and its image reconstructed. The image of the entire 3-dimensional object is obtained by putting all the reconstructed $x-z$ planes together.

The tomograms reconstructed in DT suffer from a number of artifacts:

1. Blurrings produced by objects on the off-focus planes

These blurrings can be neglected if the number of object planes involved is small and they are also spaced far apart. If these conditions are not met the blurrings will become serious.

Quantitatively consider the situation in which the object $f(x, z)$ resides on a number of planes $z = z_1, z_2, \ldots, z_n$. The tomogram $t(x, z_i)$ on the plane $z = z_i$ is given by

$$t(x,z_i) = f(x, z_i) + \sum_{j \neq i} h(x, z_i, x', z_j)\, f(x', z_j) \qquad (1)$$

where $h(x, z_i, x', z_j)$ is the blurring produced on the tomogram at the location (x, z_i) by a point object located at (x', z_j), and is given by the equation

$$h(x, z, x', z') = \begin{cases} |z-z'| / [(x-x')^2 + (z-z')^2] & \text{if } |x-x'| / |z-z'| \leq \tan\theta_0 \\ 0 & \text{otherwise} \end{cases} \qquad (2)$$

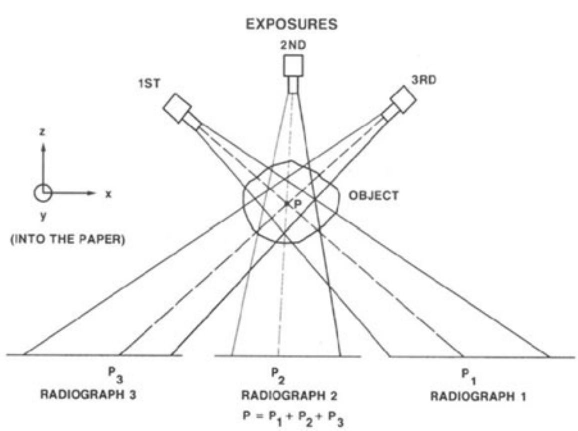

Figure 2. Conventional digital tomography in x-ray scanning.

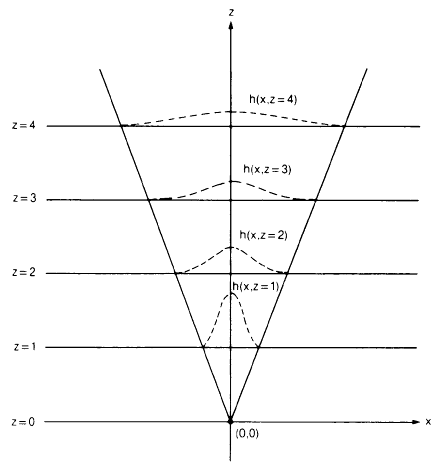

Figure 3. Blurring function or point spread function in DT.

where $2\theta_0$ is the angular coverage of the x-ray scanning. In literature this function is referred to as the point spread function. The first term on the right-hand side of Equation 1 represents the true image, and the second term represents the blurring. It can be seen that the blurring produced on a tomogram by the object $f(x',z_j)$ on another plane depends on both the magnitude of that object and the spacing between the plane and the tomogram; the latter in turn determines the magnitude of the point spread function $h(x-x',z_i-z_j)$.

The point spread function in Equation 2 can be graphically illustrated as shown in Figure 3. When the separation $|z_i-z_j|$ between the planes is small, the blurring is localized in spatial extent but large in magnitude; when the separation is large, the blurring spreads out and decrease in magnitude. Therefore the most serious blurrings come from the adjacent planes.

2. Fall off in density at the edges of the image

This effect is caused by the nonuniformity of the blurrings. The blurring is more intense at the center of a tomogram than at the edges, as illustrated in Figure 4. Because the tomogram is the sum of the real image and the blurring, it appears to be darker at the center than at the edges.

Note that the above artifacts cannot be removed by taking more radiographs or by increasing the scanning angular range. Indeed from Figure 4 it is obvious that the number of radiographs does not affect the edge effect. In fact the figure shows that the edge effect actually becomes more serious when the scanning angular range increases, as also observed in the results reported in Reference 3. Figure 5 shows that the effect of more radiographs is to make the blurring more uniform rather than to eliminate it; increasing the scanning angular range serves only to increase the spatial extent of the blurring.

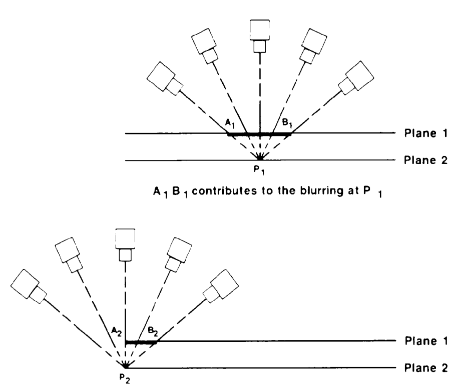

Figure 4. Edge fall-off effect.

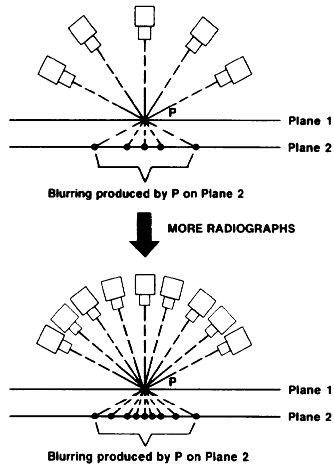

Figure 5. The effect of increasing the number of radiographs on blurring.

Several attempts were made to remove the blurrings in the tomograms. In one such attempt, the tomograms are high-pass filtered to sharpen the image [3]. The underlying assumption is that the blurrings contain mostly low-frequency components, i.e., large features. Unfortunately this is not a valid assumption. In fact, Equation 2 and Figure 3 show that only the relatively unimportant blurrings coming from planes far away spread out in spatial extent and therefore are predominantly low-frequency. On the other hand, the most serious blurrings, those coming from the adjacent planes, spread out only slightly and therefore contain pretty much the same frequency content as the objects on those off-focus planes that cause the blurrings. If the objects on those planes contain high frequency components, such as fine details and sharp features, the blurrings caused by them will also contain high-frequency components, and therefore high-pass filtering is not capable of removing them.

From these considerations we can conclude that conventional DT is at best an approximation method. It produces good images only when the planes containing the objects are far apart. Indeed, the images obtained in DT that are published in literature usually have their object planes separated by a large spacing compared to their pixel size: typically 10 pixel size apart [3]. In contrast, in applications such as the inspection of multilayer circuit boards the circuit layers are typically spaced apart by a distance which is only 2 to 3 times the pixel size. When the planes are spaced so close together, blurring becomes very serious in the conventional DT images.

This is illustrated in the following simulation results. Figure 6 shows part of the computer-generated plantom which is chosen to simulate the geometry of typical multilayer printed circuit boards. The plantom is made up of 16 layers of copper conductors. The copper wires on each layer are parallel to each other, and the wires on consecutive layers run perpendicular to each other. Each layer is 40-μm thick, and the wire is 80-μm wide with a gap of 80 μm between the wires. Adjacent copper layers are separated by a gap of 80 μm, i.e., the spacing between the centers of the layers is 120 μm. The gaps between the copper wires and between the layers simulate the unabsorbing embedding material, such as fiberglass. The density of the copper wires is assumed to be 1, and that of the embedding material assumed to be 0.

Figure 7 shows the images of layers 9 and 10 reconstructed with the conventional DT method. The input radiographs were simulated from -60° to +60° at 1° intervals. The pixel size is 40 μm × 40 μm. The wire patterns in the images completely overlap and cannot be resolved. One cannot tell in which direction the copper wires run. In addition to the blurrings, the edge fall-off effect is also apparent in these pictures: the density falls off near the top and the bottom edges of the images. There is no hope of tracing the circuits from images of such quality.

The effect of increasing the angular range of the radiographs on conventional DT is illustrated in Figure 8, where the reconstructed images of layers 9 and 10 from radiographs spanning from -80° to +80° at 1° intervals are shown. The increased angular range of the radiographs does not benefit the quality of the reconstructed images.

In passing it should be noted that the relatively high-quality DT images reported in literature were usually obtained under rather favorable conditions. The favorable conditions are: (1) large spacing

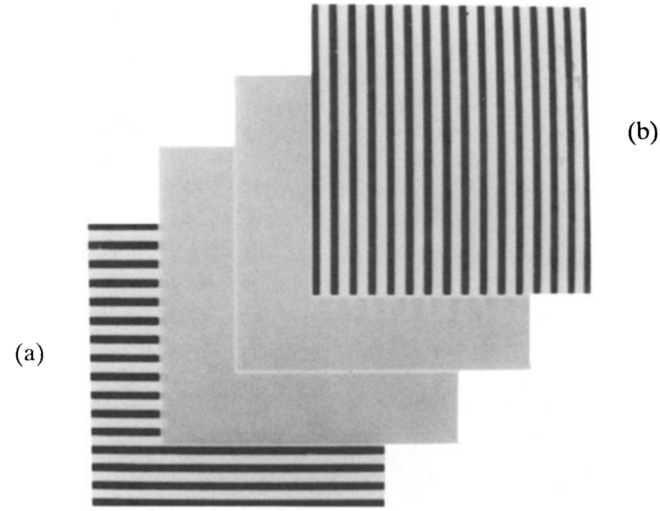

Figure 6. Part of the simulated phantom with perpendicular wire layers: layer 9 (a) and layer 10 (b).

between the planes of the tomograms; and (2) similarity between the shape of the objects on adjacent planes. For example, the plantom used in the simulations in [3] has a spacing between the planes equal to 10 times the pixel size, and the pinstripe patterns are rotated by only 22.5° from one plane to the next. Indeed, when we increase the spacing between the centers of the layers in our plantom to 10 times the pixel size, i.e., with a gap of 720 μm between the layers, and arrange the wire patterns so that the wires on adjacent layers are parallel to each other, as shown in Figure 9, we obtain the good DT images in Figure 10. Unfortunately, these favorable conditions do not meet the requirements called for in the inspection of multilayer printed circuit boards, in which the layers are closely spaced and the objects on adjacent layers are often very different in shape.

LIMITED-ANGLE IMAGE RECONSTRUCTION

It can be easily seen that the tomogram on each $x-z$ plane is the backprojection image of the object on that plane constructed from the x-ray projection data in the limited angular range. An iterative algorithm for reconstructing the object from limited-angle projection data was developed in earlier works [4,5]. The algorithm is sketched in Figure 11. It makes use of the available a priori information on the object – such as its spatial boundary, the upper bound and lower bound of its density value – to compensate for the missing scanning data. The underlying principle is that because the object $f(x,z)$ has a finite spatial extent, its Fourier transform is an analytic function, and such a function is uniquely determined if its value is known over a finite range of values. The object is transformed back and forth between the object space by filtered backprojection, and the projection space by projection, being repeatedly corrected in the object space by a priori information about the object in the object space, and by the input projection data in the projection space.

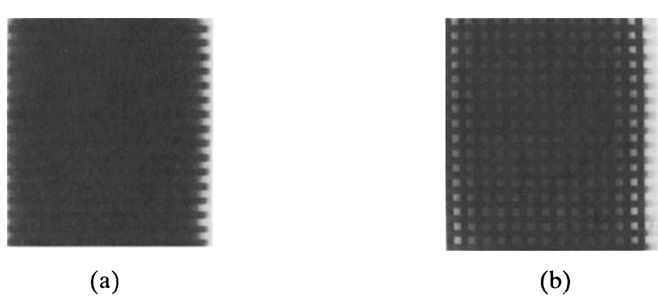

Figure 7. Images of layer 9 (a) and layer 10 (b) of the phantom in Figure 6 reconstructed with the conventional DT method; scanning angular range = 120°.

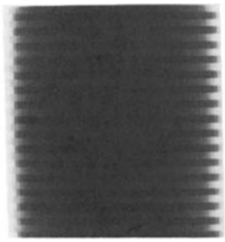

(a)

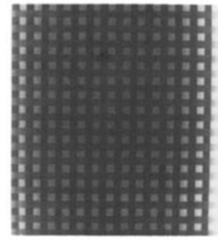

(b)

Figure 8. Images of layer 9 (a) and layer 10 (b) of the phantom in Figure 6 reconstructed with the conventional DT method; scanning angular range = 160°.

Unlike the conventional DT reconstruction method, which does not benefit from adding more radiographs or increasing the scanning angular range, the limited-angle reconstruction algorithm will yield better and better images if either the number of radiographs or their angular range is increased. The information contained in the additional radiographs is utilized efficiently by the new algorithm to improve the quality of the reconstructed images [4,5].

The limited-angle reconstruction algorithm was applied to reconstruct the simulated planton in Figure 6 (with a spacing of 80 μm between the layers). The images reconstructed from the 120° range and 160° range of radiographs, respectively, are shown in Figures 12 to 13; the input data for reconstruction are the same as those used in reconstructing the conventional DT images in Figures 7 and 8, respectively. The wire patterns are clearly resolved in these reconstructed images. The blurrings from other layers are eliminated. No edge effects are noticeable. The images can be used for circuit tracing. Also, the images reconstructed from 160° of radiographs are clearly better than the ones reconstructed from 120° of radiographs, demonstrating that the improved DT algorithm benefits from the increase in the angular range of the radiographs, as mentioned above.

SUMMARY AND DISCUSSIONS

In conclusion we summarize the comparison between the conventional DT reconstruction algorithm and the limited-angle image reconstruction algorithm as follows:

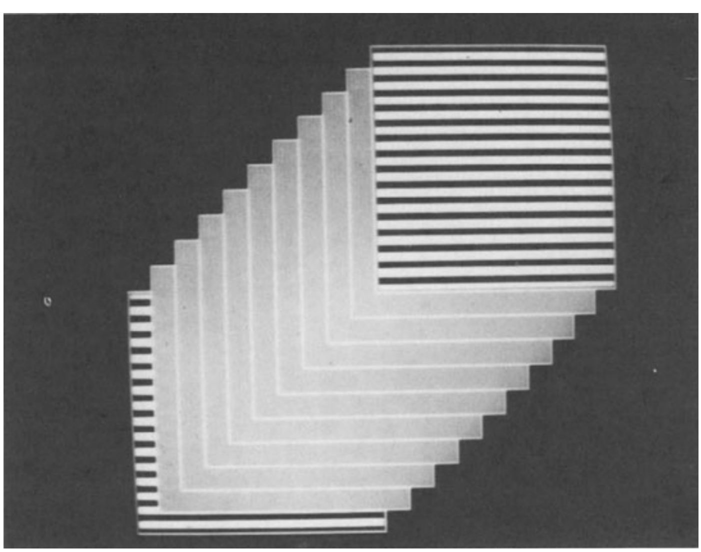

Figure 9. Part of the simulated phantom with parallel wire layers.

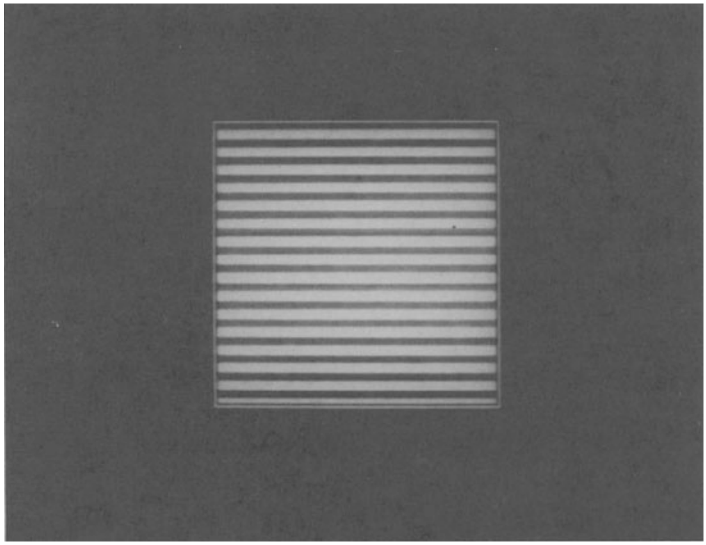

Figure 10. Image of layer 9 of the phantom in Figure 9 reconstructed with the conventional DT method.

A. Conventional DT method

1. Images blurred by objects on other planes.
2. Image density falls off near the edges.
3. Image cannot be improved by increasing either the number of radiographs or their angular range.

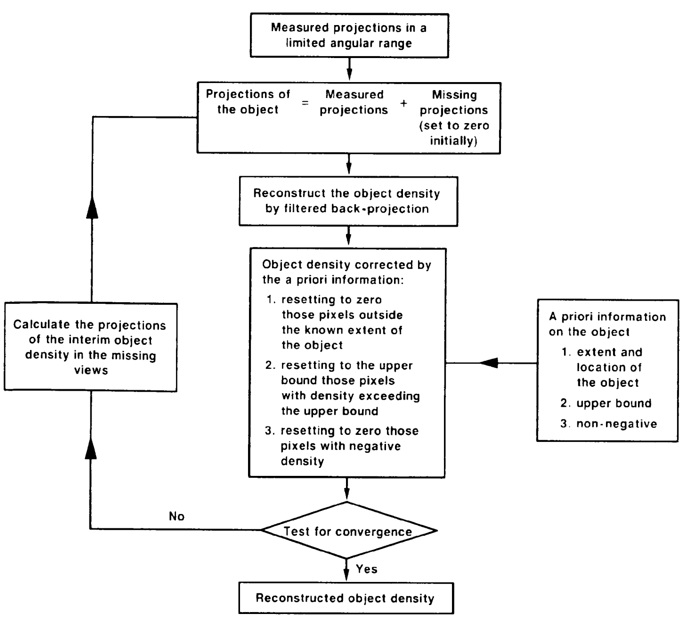

Figure 11. Limited-angle image reconstruction algorithm.

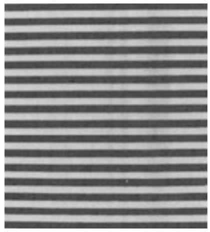

(a)

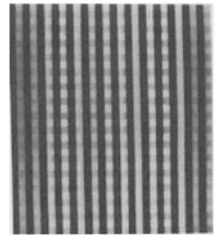

(b)

Figure 12. Images of layer 9 (a) and layer 10 (b) of the phantom in Figure 6 reconstructed with the improved DT method; scanning angular range = 120°.

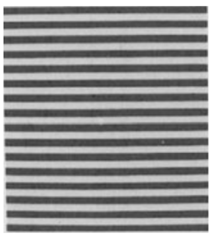

(a)

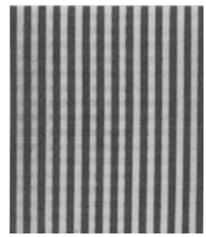

(b)

Figure 13. Images of layer 9 (a) and layer 10 (b) of the phantom in Figure 6 reconstructed with the improved DT method; scanning angular range = 160°.

B. Limited-Angle Image Reconstructions

1. Reduces blurring from other planes.
2. Does not suffer from the edge fall-off effect.
3. Image can be further improved by increasing either the number of radiographs or their angular range.

ACKNOWLEDGMENT

K.C. Tam would like to thank his wife, Brenda, for preparing the manuscript.

REFERENCES

1. S.F. Buchele, "Quantitative Computerized Laminography", in *Review of Progress in Quantitative NDE,* University of California, San Diego, July 31-August 5, 1988.
2. M. D. Barker, "Laminographic Reconstruction From Real-Time Radiographic Images", in *Review of Progress in Quantitative NDE*, University of California, San Diego, July 31-August 5, 1988.
3. J.H. Stanley, J.L. Chambers, and M.J. Boyle, "A New NDE Capability For Thin-Shelled Structures", AFWAL-TR-84-4120.
4. K.C. Tam, V. Perez-Mendez, and B. Macdonald, "3-D Object Reconstruction in Emission and Transmission Tomography with Limited Angular Input", *IEEE Trans. Nucl. Sci.*, NS-26, p.2797, 1979.
5. K.C. Tam and V. Perez-Mendez, "Tomographical Imaging with Limited-Angle Input", *J. Opt. Soc. Am., 71*, p. 582, 1981.